WELDING RESEARCH

SUPPLEMENT TO THE WELDING JOURNAL, JANUARY, 1986

Sponsored by the American Welding Society and the Welding Research Council

Readers are advised that all papers published in the *Welding Journal's* Research Supplement undergo Peer Review before publication for: 1) originality of the contribution; 2) technical value to the welding community; 3) prior publication of the material being reviewed; 4) proper credit to others working in the same area; and 5) justification of the conclusions based on the results.

The names of the more than 160 individuals serving on the AWS Peer Review Panel are published periodically. All are experts in their respective technical areas, and all are volunteers in the program.

Chemical Composition Effects on the Creep Strength of Type 308 Stainless Steel Weld Metal

Strength and ductility improve with experimental alloy GTA filler metal

BY R. L. KLUEH AND D. P. EDMONDS

ABSTRACT. Alloying additions of titanium, boron, and phosphorus are known to affect the elevated-temperature strength and ductility of austenitic stainless steel weld metals. We studied the effect of these elements on the creep-rupture properties of type 308 stainless steel. Creep-rupture tests were made at 649°C (1200°F) on specimens taken from gas tungsten arc welds deposited by use of commercial and experimental welding filler wires. Additions of about 0.4 and 0.8% Ti to the commercial composition for type 308 stainless steel increased its strength and ductility over those of welds made with a commercial filler wire. The 0.4% Ti alloy had better strength and ductility. Although small additions of boron and phosphorus had only a minor effect on strength and ductility when added to the commercial composition, separately or in combination, the addition of approximately 0.006% B and 0.042% P to a 0.4% Ti alloy significantly increased its strength above that of the 0.4% Ti alloy without boron and phosphorus.

Research sponsored by Breeder Technology Projects, U.S. Department of Energy, under contract with Martin Marietta Energy Systems, Inc.

R. L. KLUEH is with Oak Ridge National Laboratory, Oak Ridge, Tenn. D. P. EDMONDS is with Babcock and Wilcox Research and Development Division, Alliance, Ohio.

Introduction

Stress-rupture fractures of austenitic stainless steel welds often occur with low ductile weld metals. As a result, *ASME Pressure Vessel and Piping Code* Case N-47 allows only one-half the deformation permitted for similar wrought alloys. Furthermore, the creep-rupture strengths of weld metals are often less than those of wrought base metals with similar compositions.

Over the past several years, a research program to develop appropriate weld metals with improved strength and ductility was conducted (Refs. 1–4). Initial work on type 308 shielded metal arc welds showed that titanium from titania and lime-titania electrodes favorably affected the creep-rupture properties (Refs. 1,2). Special electrodes, prepared by a commercial manufacturer, were used to study chemical composition effects on type 308 stainless steel weld metal.

The results of those studies indicated the following (Refs. 1,2):

1. An increased carbon concentration caused an increase in creep-rupture strength and a decrease in ductility.
2. A reduction in silicon caused an increase in ductility with little effect on strength.
3. An increase in phosphorus caused an increase in rupture life and an improvement in ductility.
4. Sulfur had little effect on properties.
5. An increase in boron increased rupture life and ductility.

Results on shielded metal arc type 316 stainless steel welds indicated similar chemical composition effects. These studies led to the development of controlled residual element (CRE) electrodes

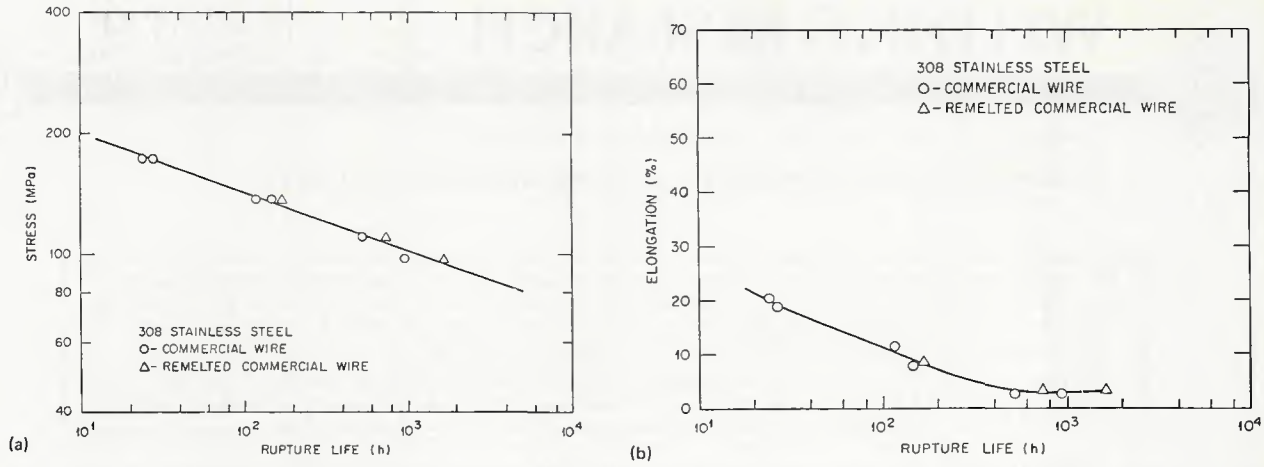

Fig. 1—Commercial type 308 stainless steel weld metal tested at 649°C. A—Stress-rupture curve. B—Total elongation plotted against rupture life

that yield weld metal deposits with nominally 0.05% Ti, 0.04% P, and 0.006% B.

In this paper, we describe efforts to determine optimum compositions for gas tungsten arc (GTA) welding wire. Studies on the effect of chemical composition on mechanical properties and microstructure were conducted in an effort to understand the strengthening mechanisms involved so that, if possible, these mechanisms can be applied to other alloy systems and welding consumables made for other processes.

Experiment

Small experimental heats of type 308 stainless steel were melted, cast, and fabricated into 3.2 mm (0.125 in.) diameter welding filler wire. Selected additions of P, B, Si, and Ti were made to these heats to determine the effect of these elements on the creep-rupture behavior and ductility of the weld metal.

A stress-rupture curve was determined for type 308 stainless steel weld metal deposited from a commercial heat of filler metal wire—Fig. 1. Some of this wire was remelted and fabricated by the same techniques used to compare the experimental heats.

Initial tests indicated that the 0.05% Ti level that had a significant effect on the strength and ductility of the shielded metal arc welds had little effect on the GTA welds. As a result, type 308 stainless steel weld deposits with nominally 0.5 and 1.0% Ti additions (the 1% alloy contained 0.9% Ti) were obtained and tested. Tests were also made on type 308 stainless steel weld metal with essentially no Si and with 0.6% Si.

Table 1 gives the chemical compositions of the heats tested. For each of the experimental heats, we determined a stress-rupture curve at 649°C (1200°F).

All the test welds were made on 13 mm (0.51 in.) thick stainless steel plates in a 75° included angle V-groove joint. The type 308 stainless steel welds were made on type 304 plates. The welds were made by the manual GTA process and stringer bead techniques with average welding conditions of 190 A and 17 V (direct current electrode negative). Eleven weld passes filled the groove. All welds used pure argon shielding gas flowing at approximately 30 cfh (14.2 L/min) using a cup-size No. 8 (½ in./12.7 mm diameter). This flow rate was found to shield the molten weld puddle without excessive cooling.

Specimens of all-weld metal 3.2 mm (0.125 in.) in diameter by 28.6 mm (1.13 in.) long parallel to the welding direction were machined from each test weld. The center of each specimen coincided with the middle of the weld about 5 mm (0.2 in.) below the top surface of the weld. These specimens were tested at 649°C (1200°F) at stress levels intended to produce rupture at 10 to 100 to several thousand hours. The load was applied gradually by mechanical and/or hydraulic devices. Extensometers mounted on the grips were used to monitor creep strains to within ±1%, and the total elongation and reduction of area were measured directly by fitting the fractured specimens together. Rupture data only are considered in this report.

Results

The beneficial effects of titanium were obvious—both the strength and ductility were significantly improved over those of the commercial steel—Fig. 2. The strength and ductility values of the 0.5% Ti alloy were higher than those of the 0.9% Ti material. Silicon had little effect on either strength or ductility. The strength of the welds with and without silicon additions fell slightly below the weld deposited with the commercial filler wire, whereas the ductility (even with 0.6% Si) was better than that of the commercial deposits—Fig. 2.

We determined the effects of boron and phosphorus relative to the commercial alloy (Fig. 3) and found that the

Table 1—Chemical Composition of Experimental Type 308 Stainless Steel Filler Metal

	Composition (wt %)								
Filler metal[a]	Cr	Ni	Mo	C	B	P	Ti	Si	Mn
Commercial heat D1773081	21.2	9.8	0.17	0.024	0.0005	0.018	<0.02	0.58	1.55
Commercial remelt	21.5	9.9	0.02	0.026	0.007	0.013	<0.01	0.48	1.59
No Si	21.5	9.9	0.04	0.026	0.002	0.035	<0.01	0.02	1.95
0.60% Si	21.5	10.0	0.03	0.026	0.002	0.025	<0.01	0.58	1.88
0.007% B[b]	21.7	10.0	0.02	0.029	0.003	0.012	<0.01	0.49	1.58
0.015% B[b]	21.5	9.9	0.02	0.026	0.007	0.013	<0.01	0.48	1.59
0.045% P	21.5	9.9	0.02	0.026	0.001	0.045	<0.01	0.48	1.58
0.06% P	21.3	9.9	0.02	0.038	0.001	0.049	<0.01	0.48	1.59
0.045% P, 0.007% B[b]	21.5	9.9	0.01	0.026	0.003	0.051	<0.01	0.50	1.55
0.5% Ti	21.5	9.9	0.02	0.026	0.001	0.012	0.49	0.52	1.55
1.0% Ti[b]	21.3	10.1	0.03	0.033	0.001	0.012	0.88	0.55	1.56
0.042% P, 0.006% B, 0.5% Ti	21.1	10.1	0.05	0.028	0.006	0.041	0.47	0.58	1.57

[a]Nominal intended compositions.
[b]Actual composition was less than aim.

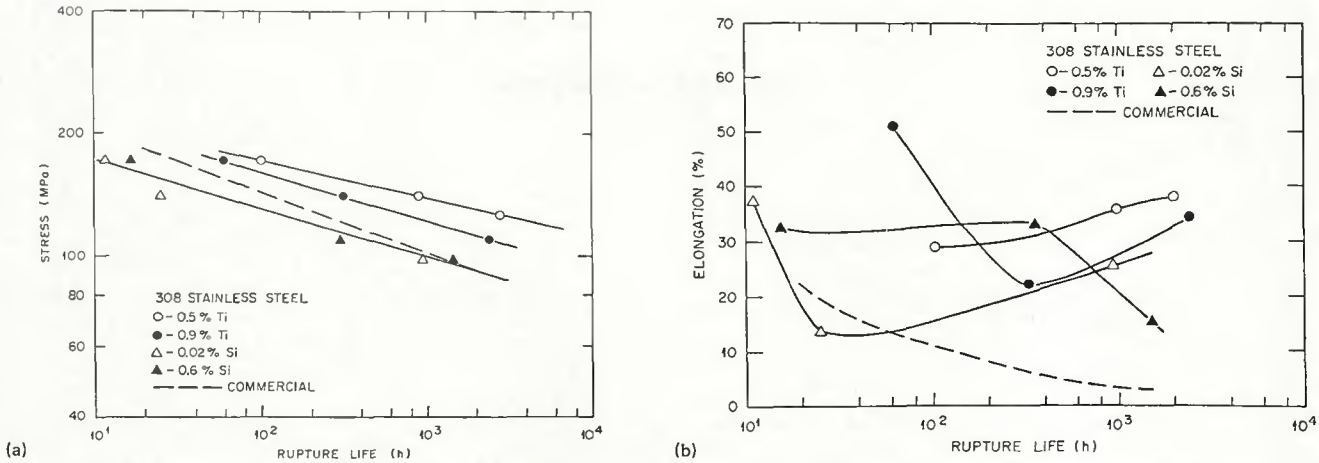

Fig. 2 — Experimental heats of type 308 stainless steel weld metal with silicon and titanium additions tested at 649°C. A — Stress-rupture curves. B — Total elongation plotted against rupture life

strength and ductility improvements were much less than those obtained with titanium additions. In contrast to the alloys in which boron or phosphorus were added separately, the alloy that contained them in combination led to the strongest and most ductile material for the longtime tests of these alloys — Fig. 3.

The above results indicated that titanium and the combination of boron and phosphorus have favorable effects on creep-rupture strength and ductility at 649°C (1200°F). These elements were combined in a heat that contained approximately 0.5% Ti, 0.006% B, and 0.041% P. This alloy was considerably stronger than the alloys with only titanium or with 0.006% B and 0.041% P — Fig. 4. The ductility varied considerably (Fig. 4B); however, even for the 3000 h test, the elongation was almost four times that of the commercial alloy.

Visual examination of the fractured specimens was in agreement with the ductility measurements. The specimens from the welds made with the commercial filler metals (as received and remelted) had flat fractures (little or no neck formation). On the specimens from the welds made with the as-received commercial filler wire, we found indications of cracks on the external surface. The specimens with nominally 0.02 and 0.6% Si were quite ductile and necked during deformation and fracture. All the low-silicon specimens showed considerable necking at all stresses, but the amount of necking decreased with decreasing stress for the 0.6% Si specimens.

Fractures for the welds made with alloys to which boron and phosphorus were added separately were quite flat (no neck formation). For the specimens from the weld containing 0.045% P and 0.003% B, we found a small amount of necking for the high-stress test but essentially none at the lowest stress.

The fractured specimens from the welds with the titanium additions displayed considerable ductility. All the 0.5 and 0.9% Ti alloy specimens tested necked during fracture. For the specimens of the weld metal that contained 0.041% P, 0.006% B, and 0.5% Ti, all specimens necked, although the necking decreased with decreasing stress. The amount of necking was less than that for specimens from welds having only titanium added.

The ferrite content of the different welds was determined with a ferrite scope on as-welded material and after exposure in a creep test at 649°C (1200°F) — Table 2. The latter measurements were made on the buttonheads of selected creep-test specimens. With a few exceptions, the ferrite number was approximately 12 to 13. Exceptions were the silicon heats, which had somewhat lower values (near 9), and the titanium heats and the heat with boron, phosphorus, and titanium added, for which larger values were obtained (18 to 23).

If the chemical compositions of the alloys are examined (Table 1), the only way to account for the difference in ferrite number for the silicon alloys is the fact that both of these heats contain somewhat more manganese than the other alloys (manganese is an austenite-stabilizing element). The high ferrite numbers of the two titanium alloys can be

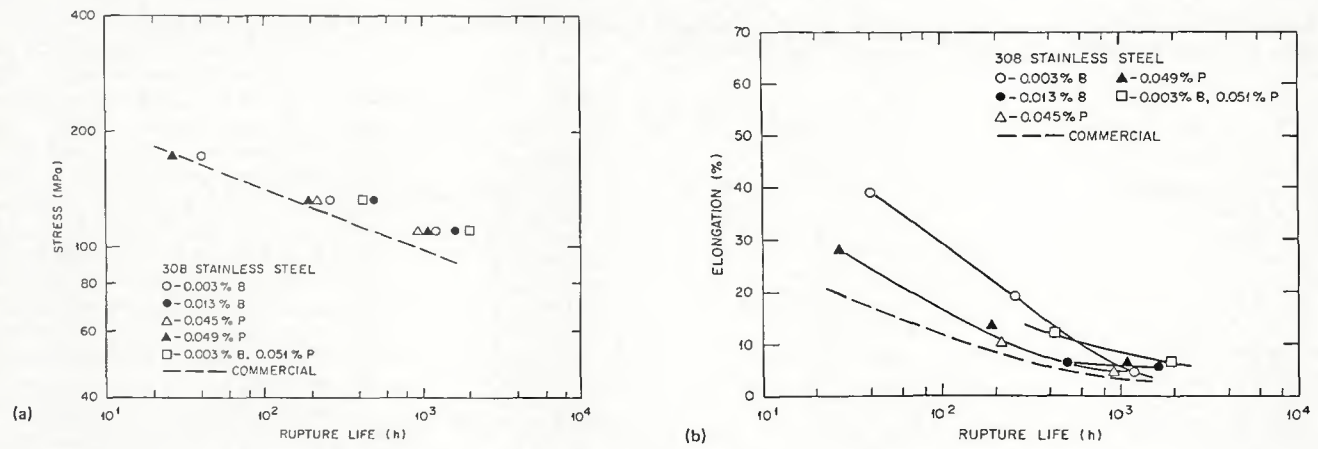

Fig. 3 — Experimental heats of type 308 stainless steel weld metal with boron and phosphorus additions tested at 649°C. A — Stress-rupture data. B — Total elongation plotted against rupture life

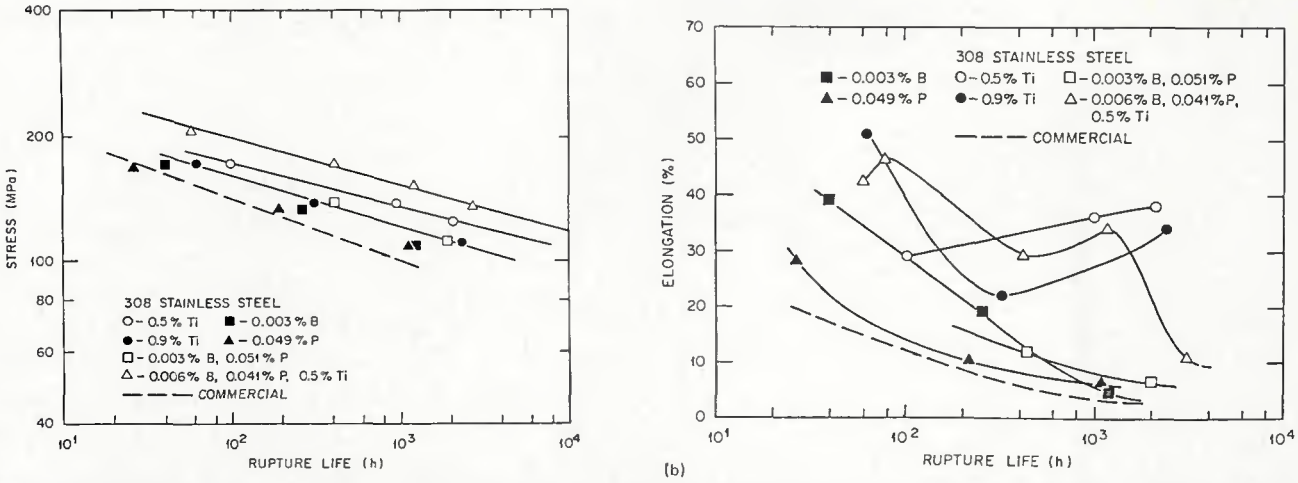

Fig. 4 — Experimental heats of type 308 stainless steel weld metal with different combinations of boron, phosphorus, and titanium tested at 649°C. A — Stress-rupture curves. B — Total elongation plotted against rupture life

attributed to titanium, a ferrite-forming element (titanium also ties up carbon and nitrogen, austenite formers). The reason for the lower ferrite number for the alloy with boron, phosphorus, and titanium additions, as compared with the alloys to which only titanium had been added, is not immediately obvious, although the difference is probably attributable to boron (boron is an austenite former, phosphorus, a ferrite former; a small effect of boron, relative to the commercial alloy, is seen in Table 2, whereas there is little effect from the phosphorus).

The decrease in ferrite number after testing is attributable to the transformation of unstable ferrite to austenite, nonmagnetic intermetallic phases, and nonmagnetic carbides (Ref. 5). Table 2 shows that the decrease in ferrite number depends on the amount of time the creep specimen was at 650°C (1200°F). It also shows that the same low number is reached by all of the alloys, regardless of the composition. If this change is caused by a partial transformation to the brittle sigma phase, as is expected, more sigma could form in the three alloys that contain titanium. Yet, these alloys are the strongest and the most ductile.

When the weld microstructures were examined, minor differences were detected in substructures — Fig. 5. The welds were first etched with a solution that attacks the polished surface in such a way that ferrite, austenite, sigma phase, and carbides can be distinguished (the etching solution is 15 g $K_4Fe(CN)_6$, 15 g KOH, and 100 mL H_2O, and is commonly known as Murakami's etchant). The specimens were then etched with aqua regia (five parts concentrated HCl to one part concentrated HNO_3) to bring out the general microstructure. The microstructures revealed by the two etchants are similar, although the aqua regia etch attacks the surface more severely and may tend to give an impression that more δ-ferrite is present than actually is. The discussion of the as-welded microstructures will assume that primarily austenite and δ-ferrite were present. This ignores the fact that for such multipass welds, some of the δ-ferrite can transform to an intermetallic phase such as sigma.

Table 2—Ferrite Number for Type 308 Stainless Steel Experimental Welds

Weld	Average ferrite number: As welded	Average ferrite number: After creep tests[a]
Commercial (V-6)	13.0	0.5 (927)
Commercial remelt (V-14)	13.0	0.8 (2084)
No Si (V-10)	9.1	0.9 (937)
0.6% Si (V-11)	9.7	0.2 (1497)
0.003% B (V-8)	12.3	0.4 (1199)
0.013% B (V-13)	11.9	0.3 (1655)
0.045% P (V-12)	12.5	0.1 (9221)
0.049% P (V-9)	12.3	0.2 (1092)
0.051% P, 0.003% B (V-16)	12.8	0.1 (1980)
0.5% Ti (V-15)	20.9	0.2 (2084)
0.9% Ti (V-7)	23.9	1.3 (321)
0.006% B, 0.041% P, 0.5% Ti (V-130, 131)	17.8	2.4 (34), 0.2 (1708)

[a]Number in parentheses is duration (hours) of creep test for specimen from which the ferrite number was determined.

Most of the ferrite in the alloys formed as laths or needles (the dark-etching phase in Fig. 5). However, the regions containing the lath structure were usually surrounded by a narrow zone of light-etching austenite. Along with the difference in ferrite content for the different welds, the increase in ferrite content appeared to lead to a finer overall microstructure; that is, the lath spacing and the size of the lath regions surrounded by austenite both decreased.

A close examination of the as-welded microstructures indicated little or no precipitate within the austenite regions of the alloys to which only titanium was added. The alloy that contained titanium, boron, and phosphorus showed some indication of precipitation — Fig. 5F. This could mean that boron and/or phosphorus somehow affect the precipitation of titanium-rich compounds. If true, it would also explain the finer microstructure of this alloy as well as the lower ferrite number (*i.e.*, precipitation removed the ferrite-forming titanium from solution). The boron and phosphorus, either by themselves or together, had little effect on the ferrite number relative to the commercial alloy — Table 2.

The fracture morphologies of the different weld metal specimens reflected the difference in ductility and fracture modes. Intersubstructural cracking was present in the as-received commercial alloy and after remelting — Fig. 6A. The alloy with a 0.6% Si addition contained somewhat more intersubstructural cracking than without silicon, although the nature of the cracks was similar. Both the alloys to which boron and phosphorus had been added separately displayed fairly flat fractures with intersubstructural cracking. An increase in boron concentration from 0.003 to 0.007% (the intended chemistry was 0.007 and 0.015%, respectively) resulted in a decreased amount of crack formation. Considerable crack for-

mation also occurred in the two alloys to which phosphorus had been added (0.045 and 0.049% P). However, all these alloys displayed significant amounts of cracking. The alloy with both boron and phosphorus additions showed relatively little cracking, although the fractures were still quite flat.

Highly ductile fractures were observed for the steels with approximately 0.5 and 0.9% Ti. There appeared to be some crack formation in the steel with 0.5% Ti. The steel with 0.006% B, 0.042% P, and 0.5% Ti had highly ductile cup-cone fractures with no indication of intersubstructural separation.

Close examination of the failed specimens revealed an apparent correlation between the failure mechanism and the substructure. For the specimens that failed with the least ductility and contained cracks in the specimen gage length, the cracks usually occurred within the narrow light-etching regions that surround the regions containing the lath ferrite — Fig. 6A. These cracks were often at the boundaries between the austenite and the lath regions. The alloys that contained only titanium had a similar δ-ferrite morphology. However, the structure is finer and no such cracks formed — Fig. 6B. The width of the light-etching austenite that surrounds the lath regions in Fig. 6B is also narrower than it is for the alloy with cracks shown in Fig. 6A.

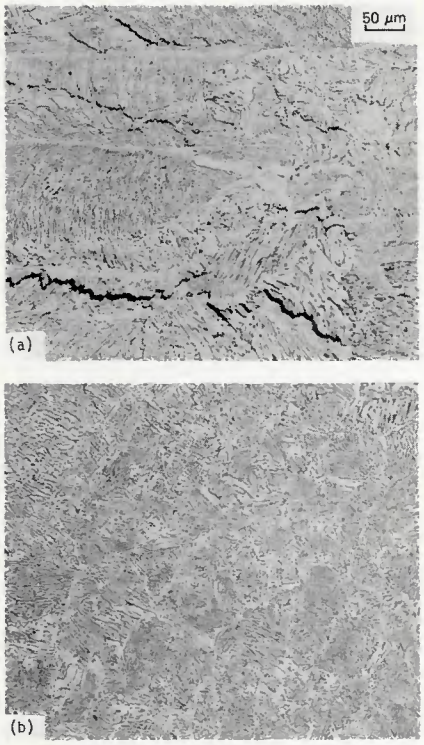

Fig. 6 — High magnification of welds showing the difference in microstructure in specimen gage sections that A — develop low-ductility intersubstructural cracks (commercial weld) and B — those that do not (0.0006% B, 0.041% P, and 0.5% Ti)

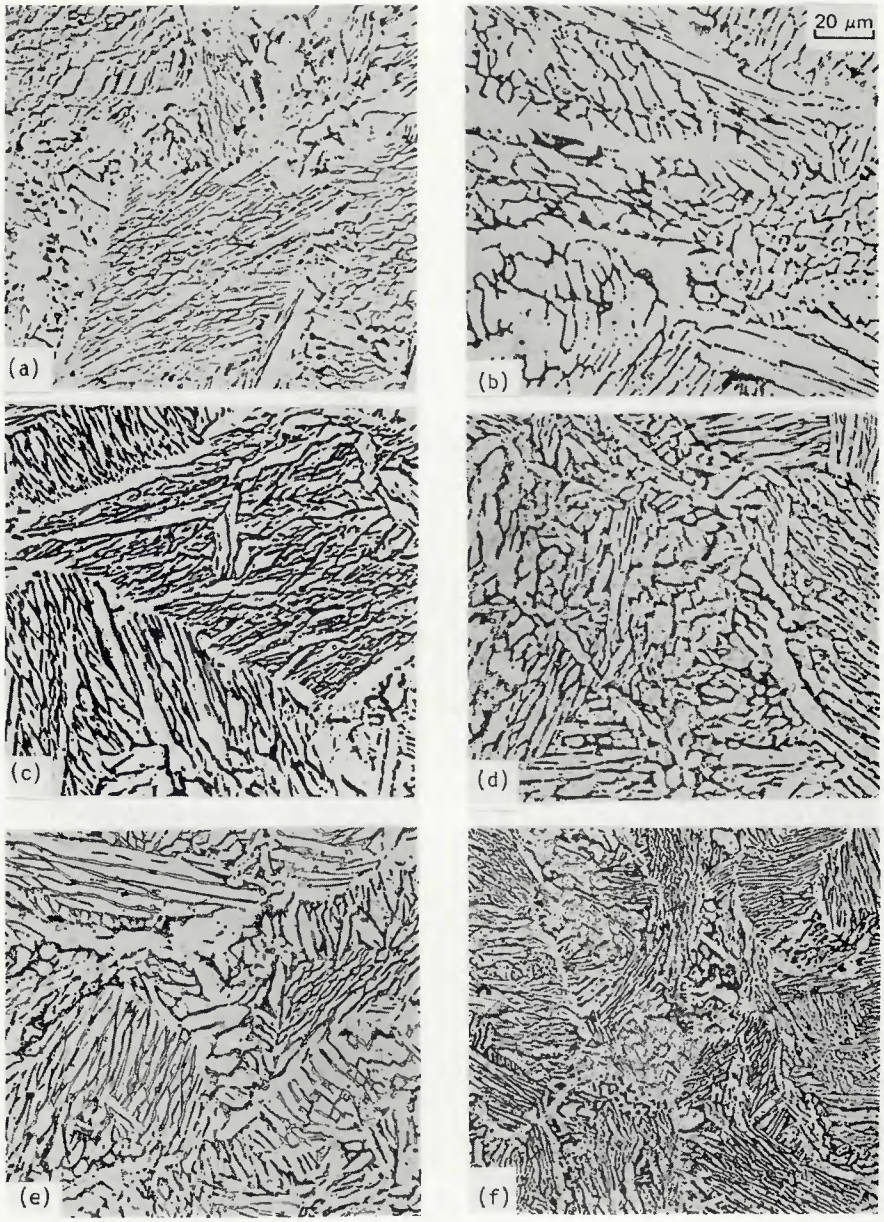

Fig. 5 — Microstructures of type 308 stainless steel weld metals. A — Commercial, B — 0.6% Si, C — 0.003% B and 0.051% P, D — 0.5% Ti, E — 0.9% Ti, and F — 0.006% B, 0.041% P, and 0.5% Ti

Discussion

The creep-rupture results from the present study are similar to those of Bloom (Ref. 6), who conducted creep-rupture studies at 700° and 815°C (1292°-1499°F) on type 304 stainless steel (chemical composition is similar to type 308 stainless steel) with 0.15% Ti and compared the results with type 304 stainless steel without titanium. When tested in the solution-annealed condition (1 h at 1038°C/1 h at 1900°F), the rupture life and ductility of the titanium-modified steel were increased significantly over the values for the unmodified alloy. A ductile transgranular fracture mode was observed for the titanium-modified steel, whereas the fracture mode of the unmodified steel was intergranular and much less ductile than the modified steel. All these observations are similar to the effect of titanium noted for the weld metals.

Transmission electron microscopy studies by Bloom (Ref. 6) revealed that during a creep test of the solution-annealed titanium-modified type 304 stainless steel, very fine titanium carbides precipitated on dislocations, thus locking them and increasing the strength. When aged before testing, most of the carbides precipitated on grain boundaries. In the unmodified alloy, most of the precipita-

tion ($M_{23}C_6$) was confined to grain boundaries; the substance in the matrix consisted of a relatively few large globular precipitates (Ref. 6). The similarity of the effect of titanium on base metal and weld metal appears to indicate that titanium plays a similar role in both.

Vitek and David (Ref. 7) recently reported on thermal aging studies on commercial type 308 stainless steel and 308CRE stainless steel to which titanium, boron, and phosphorus additions had been made. From detailed differential-thermal analysis and analytical electron microscopy studies, they concluded that there were no microstructural differences in the as-welded structures that could be used to explain the differences in creep-rupture properties. When aged between 550° and 850°C (1022° and 1562°F) for up to 10,000 h, it was found that sigma-phase formation was not retarded by the CRE additions. They found, however, that extensive precipitation of $M_{23}C_6$ occurred at the austenite-ferrite interface in the aged 308 stainless steel, whereas titanium-rich carbides, nitrides, and sulfides formed throughout the 308CRE microstructure. Vitek and David (Ref. 7) proposed that it is the elimination of the continuous network of $M_{23}C_6$ carbides that is responsible for the improved elevated-temperature creep-rupture properties of the CRE weld metal.

The results of the present work do not disagree with this proposal. However, this proposal does not address the effect of boron and phosphorus. As seen in Fig. 5, an addition of a combination of boron and phosphorus, titanium separately, or titanium in combination with boron and phosphorus gave rise to a finer microstructure than was obtained when the elements were absent. Furthermore, the combination of 0.003% B and 0.051% P improved the strength over that for commercial type 308 stainless steel. Although the nature of the effects is not understood, these observations indicate that the boron and phosphorus are also playing a role in the improvement of the properties, in addition to that due to the change in precipitate character caused by the titanium.

Studies on the effect of phosphorus and boron individually on the strength and ductility of type 18-8 austenitic stainless steels have been reported (Refs. 8–14). In the case of phosphorus, the concentrations studied were generally about 10 times those used in this study. It has been shown that phosphorus can augment dispersion hardening caused by carbon (Ref. 13). Several explanations have been offered. Most generally, it is concluded that phosphorus enters into the $M_{23}C_6$ in the form $M_{23}(CP)_6$ (Refs. 9, 10). It also affects the morphology of the precipitate; that is, it gives rise to a finer matrix precipitate than when phosphorus is not present (Refs. 9, 10). It is also felt that it increases ductility by leading to less grain boundary precipitates.

Rowcliffe and Nicholson (Ref. 11) studied the effect of phosphorus on precipitation in a low-carbon type 18-10 stainless steel with 0.3% P and found that, when these alloys were quenched from 1300°C (2372°F), a variety of vacancy defects were formed. They concluded that the defects were formed as a result of an interaction between vacancies and phosphorus atoms. Eventually these vacancy defects acted as nucleation sites for Cr_3P precipitates. The authors felt a similar process could be responsible for the influence of phosphorus on carbide precipitation observed in steels with higher carbon contents.

Boron has also been found to have an effect on precipitation in austenitic stainless steels. Henry and co-workers (Refs. 12–14) found that the addition of boron up to 0.015% led to a marked improvement of hot strength and room temperature ductility of 18 Cr – 12 Ni – 3 Mo (a composition similar to type 316 stainless steel). They concluded that the boron influenced the nucleation of the $M_{23}C_6$ and the subsequent interaction of this precipitate with dislocations (Refs. 12, 13). Boron was also thought to decrease the solubility of carbon in the stainless steel.

The above discussion shows that titanium, phosphorus, and boron can individually increase the strength and ductility of austenitic stainless steels. It also appears that each of these elements has a similar effect on the eventual precipitate morphology. Titanium additions lead to the replacement of relatively continuous $M_{23}C_6$ grain boundary precipitates by a fine titanium-rich precipitate, whereas boron and phosphorus promote a finer $M_{23}C_6$ precipitate. In both cases, precipitation at dislocations during creep is enhanced, thus increasing strength, and continuous grain boundary or intersubstructural precipitation is eliminated, thus increasing ductility. The exact nature of the effect of boron and phosphorus in the presence of titanium still needs to be determined.

When an austenitic stainless steel weld metal is tested in creep (or thermally aged) at 500° to 900°C (932°–1652°F), the δ-ferrite can transform to the hard, brittle intermetallic phases, such as the sigma phase (Ref. 15). Brittle fracture at the intermetallic-austenite boundary has often been attributed to sigma phase (Refs. 5, 16). Because the strength and ductility both increased with some of the changes in chemical composition that also led to higher δ-ferrite contents and presumably larger amounts of sigma, the processes are undoubtedly quite complicated. Furthermore, Vitek and David (Ref. 7) found little difference in the formation of sigma phase in the commercial type 308 stainless steel or the 308CRE to which Ti, B, and P had been added. It appears, therefore, that either the effect of sigma on the rupture behavior may be considerably less than previously thought or the finer microstructure neutralizes the effect.

Summary and Conclusions

We investigated the effect of alloying additions on the elevated-temperature strength and ductility of type 308 stainless steel weld metal by making controlled additions of Si, Ti, P, and B to the commercial composition for the filler metal. These experimental filler-metal alloys were then used to make GTA welds. Creep-rupture tests at 649°C (1200°F) were made on specimens taken from these welds.

Nominal additions of 0.5 and 0.9% Ti increased the strength and ductility of the type 308 stainless steel; the 0.5% Ti addition had the greater effect. Silicon additions to the commercial composition for type 308 stainless steel had little effect on strength and ductility. Minor additions of boron and phosphorus increased the strength slightly, but additions of the combination (0.003% B and 0.051% P) gave essentially an additive effect. This combination of alloying elements did not give effects as great as the nominal 0.5 and 1.0% Ti additions. Finally, the addition of 0.041% P, 0.006% B, and 0.5% Ti to the type 308 stainless steel composition produced an alloy with the greatest strength and ductility.

Acknowledgments

Special thanks are due to several people. E. Bolling carried out the experimental work. C. W. Houck did the metallography. The manuscript was reviewed by S. A. David and R. W. Swindeman. Susan Hancher prepared the final copy.

References

1. Binkley, N. C., Goodwin, G. M., and Harman, D. G. 1973. Effects of electrode coverings on elevated-temperature properties of austenitic stainless steel weld metal. *Weld. J.*, 52(7): 306-s to 311-s.

2. King, R. T., Stiegler, J. O., and Goodwin, G. M. 1974. Relation between mechanical properties and microstructure in CRE type 308 weldments. *Weld. J.*, 53:(7): 307-s to 313-s.

3. Berggren, R. G., et al. 1978. Structure and elevated temperature properties of type 308 stainless steel weld metal with varying ferrite contents. *Weld. J.*, 57(6): 167-s to 174-s.

4. Edmonds, D. P. 1979. Residual elements have significant effects on the elevated-tem-

perature properties of austenitic stainless steel welds. *Properties of Austenitic Stainless Steels and Their Weld Metals (Influence of Slight Chemical Variations)*, p. 56, American Society for Testing Materials, Philadelphia.

5. Edmonds, D. P., Vandergriff, D. M., and Gray, R. J. 1978. Effects of delta ferrite content on the mechanical properties of E308-16 stainless steel weld metal—III. Supplemental Studies. *Properties of Steel Weldments for Elevated Temperature Pressure Containment Applications*, p. 47, American Society of Mechanical Engineers, New York.

6. Bloom, E. E. 1967. *Effect of Titanium Additions on the Stress-Rupture Properties of Type 304 Stainless Steel.* ORNL/TM-1807, June.

7. Vitek, J. M., and David, S. A. 1984. The solidification and aging behavior of types 308 and 308CRE stainless steel welds. *Weld. J.*, 63(8): 246-s to 253-s.

8. Allten, A. G., Chow, J. G. Y., and Simon, A. 1954. Precipitation hardening austenitic chromium-nickel steels containing high carbon and phosphorus. *Trans. Am. Soc. Met.*, 45: 948-972.

9. Froes, F. H., Wells, M. G. H., and Banerjee, B. R. 1968. Influence of phosphorus on the nucleation of $M_{23}C_6$ carbides in austenitic stainless steels. *Met. Sci. J.*, 2: 232-234.

10. Irvine, K. J., Llewellyn, D. T., and Pickering, F. B. 1961. High-strength austenitic stainless steels. *J. Iron Steel Inst.*, 199: 153-175.

11. Rowcliffe, A. F., and Nicholson, R. B. 1972. Quenching defects and precipitation in a phosphorus-containing austenitic stainless steel. *Acta Metall.* 20: 143-155.

12. Henry, G., Plateau, J., Mercier, A., and Hochmann, J. 1963. Influence de faibles additions de bore sur la resistance au fluage et la structure micrographique d'aciers derivan du Type 18-10. *Rev. Metall.* 61: 1221-1232.

13. Henry, G., et al. 1974. Orientation and morphology of $M_{23}(BC)_6$ precipitates in austenite grain boundaries. pp. 666-667, *Electron Microscopy 1974*, Australian Academy of Science, Canberra, A.C.T., Australia.

14. Thomas, B. J., and Henry, G. 1980. Boron in austenitic stainless steels. *Boron in Steels*, pp. 80-105, The Metallurgical Society of AIME, Warrendale, Pa.

15. Maline, M. O. 1967. Sigma and 885°F embrittlement of chromium-nickel stainless steel weld metals. *Weld. J.*, 46(6): 241-s to 253-s.

16. Hauser, D., and Van Echo, J. A. 1978. Effect of delta ferrite content of E308-16 stainless steel weld metal—II. Mechanical Property and Metallographic Studies. pp. 17-46, *Properties of Steel Weldments for Elevated Temperature Pressure Containment Applications*, American Society of Mechanical Engineers, New York.

WRC Bulletin 307
August 1985

Fatigue and Creep Rupture Damage of Perforated Plates Subjected to Cyclic Plastic Straining in Creep Rupture

By M. L. Badlani, T. Tanaka, J. S. Porowski and W. J. O'Donnell

In this report, stress relaxation and inelastic strains accumulated in ligaments of perforated plates subjected to cyclic plastic straining, followed by creep relaxation, were analyzed. Ligaments of perforated tubesheets (plates) with triangular and square penetration patterns of circular holes, subjected to in-plane cyclic loading, were studied. Elastic follow-up is shown to occur in ligaments of perforated plates subjected to plastic cyclic straining under creep conditions.

The publication of this report was sponsored by the Subcommittee on Shells and Ligaments of the Pressure Vessel Research Committee of the Welding Research Council. The price of WRC Bulletin 307 is $12.00 per copy, plus $5.00 for postage and handling. Orders should be sent with payment to the Welding Research Council, Ste. 1301, 345 E. 47th St., New York, NY 10017.

WRC Bulletin 308
September 1985

Verification and Application of an Inelastic Analysis Method for LMFBR Piping Systems

By H. D. Hibbitt and E. K. Leung

The primary purpose of this report is to show when elbow end effects are important, and how they influence the predictions of stress and strain components in the inelastic range. The secondary purpose is to demonstrate an economical inelastic analysis method which can be used routinely to design piping systems operating at elevated temperature.

The publication of this report was sponsored by the Subcommittee on Elevated Temperature Design of the Pressure Vessel Research Committee of the Welding Research Council. The price of WRC Bulletin 308 is $14.00 per copy, plus $5.00 for postage and handling. Orders should be sent with payment to the Welding Research Council, Ste. 1301, 345 E. 47th St., New York, NY 10017.